

## Research Paper

**Cite this article:** Xu Y, Ye Q, Meng G (2018). Hybrid phase retrieval algorithm based on modified very fast simulated annealing. *International Journal of Microwave and Wireless Technologies* **10**, 1072–1080. <https://doi.org/10.1017/S1759078718000971>

Received: 22 March 2018  
Revised: 22 May 2018  
Accepted: 24 May 2018  
First published online: 22 June 2018

### Key words:

Antenna design; EM field theory; modelling and measurements; phase reconstruction

### Author for correspondence:

Qian Ye, E-mail: [yeqian@sjtu.edu.cn](mailto:yeqian@sjtu.edu.cn)

# Hybrid phase retrieval algorithm based on modified very fast simulated annealing

Yueshu Xu, Qian Ye and Guoxiang Meng

Shanghai Jiao Tong University, 800 Dongchuan Road, Minhang District, Shanghai, China

## Abstract

The Misell algorithm is one of the most widely used phase retrieval holography methods for large reflector antennas to measure surface deformation. However, it usually locks in a local minimum because it heads downhill from an initial estimation without any consideration whether it heads for a global minimum or not. The core problem of the Misell algorithm is to find an initial estimation near the global minimum to avoid local stagnation. To cope with the problem, we construct a hybrid Misell algorithm, named modified very fast simulated annealing (MVFSA)-Misell algorithm, to search for the global minimum with a high efficiency. The algorithm is based on the combination of the MVFSA algorithm and Misell algorithm. Firstly, the MVFSA is utilized to obtain a rough position near the global minimum in limited steps. Then, the Misell algorithm starts from the rough position to converge to the global minimum with high speed and accuracy. The convergence characteristic of the proposed algorithm was discussed in detail through digital simulation. Simulation results show that the algorithm can reach global minimum in a very short time. Unlike the traditional Misell algorithm, the hybrid algorithm is not influenced by initial phase estimation.

## Introduction

For large reflector antennas, the deformation of the reflector surface caused by wind, load, temperature or panels' construction will highly influence the aperture efficiency [1]. Ruze suggested that the root-mean-square-error (RMSE) deviation of the reflector surface from the ideal surface should be less than  $\lambda/15$  to obtain more than 50% aperture efficiency [2]. To maintain high efficiency in astronomy observation, large reflector antennas are equipped with an active surface system to adjust malposed panels to ideal locations [3]. The malalignments of the panels must be detected by using an effective and accurate diagnostic procedure before the panel adjustment.

Among different measuring methods for the deformation of the reflector surface, microwave holography is the most widely used and effective one. It can be divided roughly into two groups: phase coherent holography (PCH) and phase retrieval holography (PRH) [4]. PCH uses both the phase and amplitude of the beam pattern. It obtains the phase of far-field by employing the interferometric principle of phase difference measurement between two channels, but it needs additional equipment such as a reference antenna and phase-sensitive receiver. Moreover, as the operating frequencies increase, accurate phase measurements become more difficult, expensive and unreliable [5]. Unlike PCH, PRH only needs the amplitude of the beam pattern. The phase of the beam pattern is recovered by phase retrieval algorithms in PRH [6]. Therefore, PRH is a more convenient and appropriate way for high-frequency observation.

The Misell algorithm is one of the most widely used PRHs for large reflector antennas. It can realize the reconstruction of the phase distribution of the electric field in the aperture plane, from which the surface deviations can be calculated accurately. The algorithm requires two or more far-field amplitude patterns to be measured: one with the antenna in focus and the other with the antenna defocused. In the iterative calculation, the aperture phase distribution compatible with all measured patterns is determined from the defocused radiation characteristics [7]. The Misell algorithm has been applied and reported in large antennas such as UDSC-64m, TM-65m, GBT-100m, and Effelsberg-100m with considerable success [8–10].

The major problem of the Misell algorithm is that it usually stagnates in the local minimum. To avoid the stagnation, Morris studies the convergence characteristic of the Misell algorithm and concludes that the Misell algorithm is an unreliable method akin to the method of steepest decent because it heads downhill from an initial estimation without any consideration whether it heads for a global minimum or not [11]. Nieto-Vesperinas *et al.* utilize the simulated annealing in PRH and report that it needs at least 3 h to complete the reconstruction of  $32 \times 32$  pixels pattern [12]. Long computing time limits its application in the realistic astronomy observation.

In this paper, we construct a hybrid Misell algorithm, named modified very fast simulated annealing (MVFSA)-Misell algorithm, to search for the global minimum of the aperture phase. The algorithm is based on the MVFSA, which is a modification of the traditional simulated annealing (SA) introduced novel perturbation model with stronger traversal capability at the beginning of the iteration. To further enhance the global search capability, the iterative process of the MVFSA is divided into two stages and the initial temperature of the second stage is added by a given value from the end temperature of the first stage. The MVFSA is utilized to optimize the aperture phase distribution, which is parameterized by Zernike polynomials, to obtain a rough global minimum position in limited iteration steps. With the rough estimation as an initial phase, the Misell algorithm approaches global minimum with high accuracy and fast convergence speed. The MVFSA-Misell algorithm combines the powerful global search capability of the MVFSA and the superior speed of local convergence in the Misell algorithm. Analysis of algorithm performance in accuracy, speed, and initial phase effect was performed in detail through digital simulation.

This paper is outlined as follows. In section “Misell algorithm”, we review the theory of Misell algorithm. Section “MVFSA-Misell algorithm” describes the hybrid global optimization algorithm MVFSA-Misell. Simulation and analysis are presented in section “Simulation”. The conclusions are presented at the end.

### Misell algorithm

The method of reconstructing wave-front phase distribution by intensity distribution was first proposed by Gerchberg-Saxton in 1972, and the algorithm (Gerchberg-Saxton, GS algorithm) solves the phase distribution of the wave function by the iterative method from the intensity distribution on the known plane and diffraction plane. In 1973, D. Misell modeled the GS algorithm and proposed the Misell algorithm to reconstruct the phase distribution of the wave function from the intensity distribution of the two defocused images with different defocusing values. Below we introduce the principle of the Misell algorithm [7].

In the small angle far field region, which is the intersection of the small angle and far-field regions, the field distribution satisfies the following equation:

$$F(u, v) = \frac{i}{\lambda} \frac{e^{-ikR}}{R} \int f(x, y) \exp\{-ik(ux + dy)\} dx dy, \quad (1)$$

where  $f(x, y)$  represents the aperture distribution,  $R$  is the distance from the far-field point to the center of the aperture,  $\lambda$  is the wavelength, and  $k$  is the wave number, which equals  $2\pi/\lambda$ . It is illustrated that there exists a Fourier transform relationship between the aperture distribution and far-field distribution. For the convenience of discussion,  $i/\lambda$  and  $e^{-ikR}/R$  are ignored, and the aperture distribution and far-field distribution are expressed as the following equation in the form of amplitude and phase:

$$f(x, y) = |f(x, y)| \exp[i\varphi_f(x, y)], \quad (2)$$

$$F(u, v) = |F(u, v)| \exp[i\varphi_F(u, v)]. \quad (3)$$

In the case of defocus operation, it is assumed that there is an additional phase difference  $\Delta\varphi$  in the aperture field, and the

defocused aperture distribution is changed to

$$f_d(x, y) = f(x, y) \exp(i\Delta\varphi). \quad (4)$$

The relationship between the defocused and infocus far-field distributions can be expressed as follows:

$$F_d(u, v) = ft\{\exp(i\Delta\varphi) \cdot ift[F(u, v)]\} = G[F(u, v)], \quad (5)$$

$$F(u, v) = ft\{\exp(-i\Delta\varphi) \cdot ift[F_d(u, v)]\} = G^{-1}[F_d(u, v)], \quad (6)$$

where  $ft$  represents Fourier transform,  $ift$  represents inverse Fourier transform,  $G$  and  $G^{-1}$  are defined as

$$G = ft\{\exp(i\Delta\varphi) \cdot ift\}, \quad (7)$$

$$G^{-1} = ft\{\exp(-i\Delta\varphi) \cdot ift\}. \quad (8)$$

The iterative equation of the Misell algorithm is expressed as follows:

$$F_d^k(u, v) = ft\{\exp(i\Delta\varphi) \cdot ift[F^k(u, v)]\} = GF^k(u, v), \quad (9)$$

$$F_d^k(u, v) = |F_d^k(u, v)| \exp[i\Delta\varphi_{Fd}^k(u, v)], \quad (10)$$

$$F^k(u, v) = ft\{\exp(-i\Delta\varphi) \cdot ift[F_d^k(u, v)]\} = G^{-1}F_d^k(u, v), \quad (11)$$

$$F^{k+1}(u, v) = |F^k(u, v)| \exp[i\Delta\varphi_F^k(u, v)]. \quad (12)$$

The Misell algorithm starts from an estimation of the aperture distribution, and repeats (9)–(12) over and over until it satisfies the convergence criterion. The advantage of the Misell algorithm is that it can converge to the final solution with a high speed because the “projection” in (10) and (12) is an error reduction operation, which means the solution error at the  $k + 1$ th iteration is always lower than that at  $k$ th. On the other hand, if the initial estimation of the aperture distribution is far from the global minimum, the Misell algorithm will easily converge to the local minimum. The goal of this paper is to find an initial estimation near the global minimum to avoid local stagnation.

### MVFSA-Misell algorithm

To find an appropriate initial estimation of the Misell algorithm, this paper constructs a hybrid MVFSA-Misell global optimization algorithm. The algorithm is based on the MVFSA, which is an improved form of very fast simulated annealing (VFSA) by enhancing the traversal capability of the algorithm at the initial stage of iteration. Below, we introduce the principles of the VFSA and MVFSA.

In a traditional SA, a given model state with energy  $E_1$  is compared to a state which is affected by a given perturbation. The perturbation displaces one of the particles of the state to another location on a small scale. The new state, with energy  $E_2$ , is accepted if  $E_2 - E_1 \leq 0$ . However, if  $E_2 - E_1 > 0$ , it does not mean the new state is rejected. It can be accepted if  $\exp[-(E_2$

$-E_1)/T] > u$ , where  $T$  is the model temperature and  $u$  is a random number between 0 and 1. The receiving criterion is called the Metropolis criterion, which is the essence of the algorithm. The acceptance of the “deterioration” keeps the solution not stagnate at a local minimum. By repeating this process, the model temperature gets lower by a given annealing scheme. The global minimum of the state energy can be approached at a lower temperature. The SA method has been widely used because no specific information about the cost function is needed and it is easy to put into practice. However, the major problem of SA is that it costs a tremendous amount of time and computational efforts, which restricts its application in industry.

To speed up the convergence rate of SA, VFSA chooses a new perturbation model—a Cauchy-like distribution function, which is expressed as

$$g'_i(x, y) = g_i(x, y) - y_i(B_i - A_i) \\ y_i = T(u - 0.5) \left[ \left( 1 + \frac{1}{T} \right)^{|2u-1|} - 1 \right], \quad (13)$$

where  $g_i(x, y)$  represents the current model,  $g'_i(x, y)$  represents the perturbed model,  $[A_i, B_i]$  is the value range of  $g_i(x, y)$ ,  $T$  represents the model temperature and  $u$  is a random number between 0 and 1 [13]. The perturbation model is able to realize a narrower search as the iterative solution approaches optimum solution, which accelerates the convergence speed, but the traversal capability of the algorithm at the initial stage of iteration is sacrificed at the same time, which means there is a little risk of falling into the local minimum.

To enhance the global search capability of VFSA, we propose the MVFSA, which improves the VFSA in the following two aspects:

- (1) An additional iterative stage is added to examine the global solution at high temperature. The initial temperature of this extra stage is slightly higher than the final temperature of the first stage, but not higher than the initial temperature of the first stage. This gives the model a chance to jump out of the local minimum. It is also a test to determine whether the intermediate solution has been dropped in the real optimal interval during the first stage.
- (2) At the first stage, the global perturbation model replaces the current perturbation model, because the state traversal ability of random generators is higher than the special model perturbation model of the VFSA algorithm, and the global perturbation model generated by a random number is independent of the initial temperature, which means there is no need to take the value of temperature into account.

It must be pointed out that the above improvement is only the change of the annealing scheme and perturbation model. The generalized Boltzmann–Gibbs distributed receiving probability and the Metropolis criterion adopted in the algorithm are not changed, which means the global search mechanism of the SA is not changed. The expressions of the perturbation model and annealing scheme in the two stages of MVFSA are given in Fig. 1.

To avoid the local stagnation of the traditional Misell algorithm, we combine the MVFSA and the Misell algorithm to construct the global optimization algorithm MVFSA–Misell. In the MVFSA–Misell algorithm, we apply the MVFSA to get a rough

estimation of the aperture distribution near the global minimum and utilize the Misell algorithm to converge to the global minimum from the rough estimation. The flowchart of the algorithm is illustrated in Figs 2 and 3. The main steps of the algorithm can be summarized as follows:

*Step I: Achieve a rough estimation of aperture phase:* To aid in the interpretation of optical test results, it is convenient to express wave-front data in the polynomial form. In this paper, we used the Zernike polynomials to parameterize the phase distributions in the aperture. In mathematics, the Zernike polynomials are a sequence of polynomials that are orthogonal on the unit disk. They can be written as

$$Z_n^m(r) = \sum_{k=0}^{(n-m)/2} (-1)^k \frac{(n-k)!}{[(n+m-2k)/2]! [(n-m-2k)/2]! k!} r^{n-2k}, \\ r \leq 1, n > m \geq 0, n-m = \text{even}, \quad k = \frac{n-m}{2}, \quad (14)$$

where  $Z_n^m(r)$  represents the Zernike polynomial in two positive integers,  $n$  and  $m$ , and  $r$  represents the radial radius in the circular domain. The initial Zernike polynomial coefficients can be given in different forms. Then, the Zernike polynomial coefficients are optimized by the MVFSA to minimize the cost function—the RMSE of the far-field amplitudes, which is defined as

$$RMSE = \sum_{k=1}^2 \sqrt{\frac{\sum_N \sum_N (|F_{far,k}| - |F_{m,k}|)^2}{N^2}}, \quad (15)$$

where  $|F_{far,k}|$  is the calculated far-field amplitude,  $|F_{m,k}|$  is the measured far-field amplitude,  $k$  is the number of measured amplitudes, and  $N$  is the number of data points in the array. To save CPU time, the maximum iteration of MVFSA is set as a limited number. The goal of the MVFSA is just to achieve a rough estimation of the aperture phase instead of the final global minimum. The long subsequent iterative process of the MVFSA is replaced by the Misell algorithm in the next step due to the superior speed of the Misell algorithm.

*Step II: Converge to the global minimum from the rough estimation by Misell algorithm:* The step starts with a calculation of the complex infocus aperture distribution, which is composed of the optimized rough estimation of aperture phase and estimated Gaussian amplitude. Then the estimated aperture distribution is propagated into far-field by Fourier transform. There the resulting calculated far-field amplitude is replaced by the measured amplitude and the phase is retained unchanged. This modified infocus far-field amplitude and phase distribution is then propagated into aperture by inverse Fourier transform. By adding a phase factor, which connects the aperture phase error between infocus and defocused with defocusing distance, the defocused aperture pattern is solved accurately. The procedure can then iterate by propagating again to the infocus aperture plane and by repeating the cycle again and again. The convergence criterion used in this paper is defined as shown below:

$$\sqrt{\frac{1}{N^2} \sum_N \sum_N [\varphi_{in}^n(x, y) - \varphi_{in}^{n-1}(x, y)]^2} < 10^{-6}, \quad (16)$$

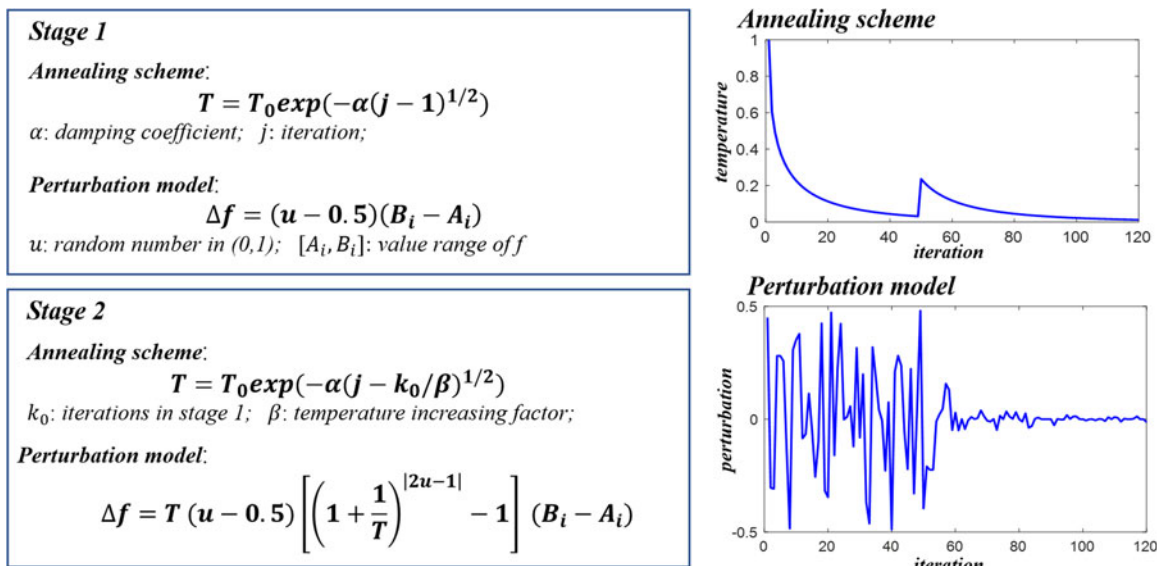


Fig. 1. Perturbation model and annealing scheme in two stages of MVFSA.

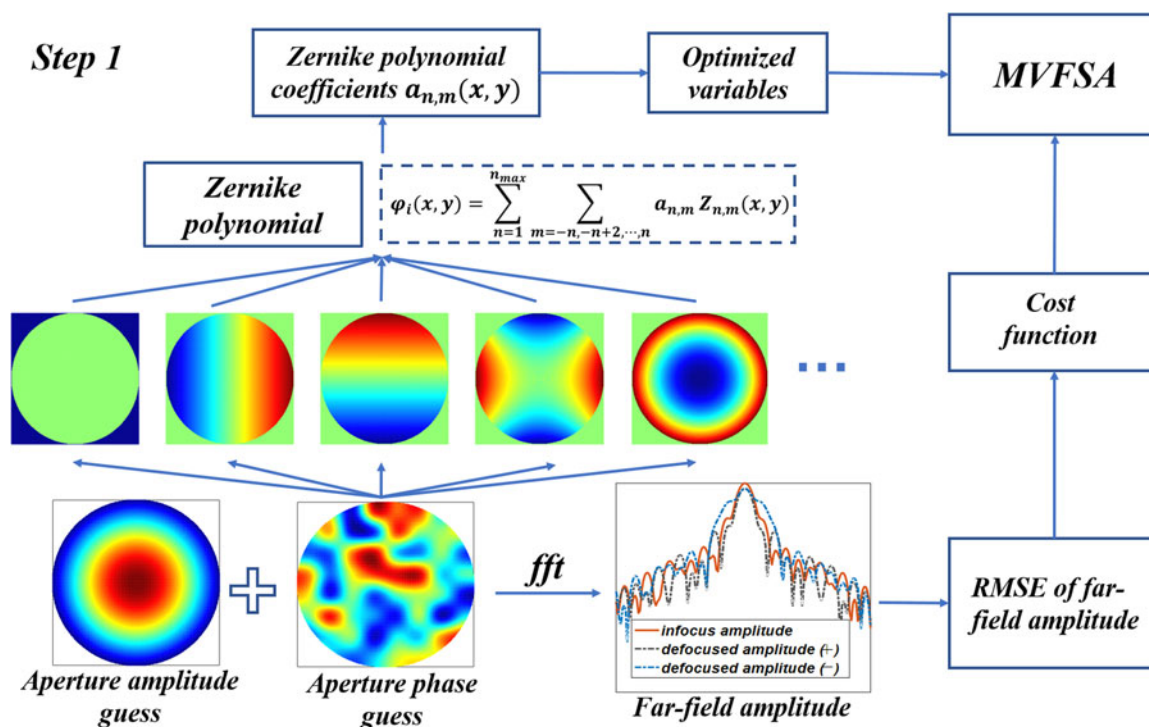


Fig. 2. Schematic diagram of step 1 of the MVFSA-Misell algorithm.

where  $\varphi_{in}^n(x, y)$  is the retrieved infocus phase distribution in an aperture at the  $n$ th iteration.

Reviewing the above steps, the method is convenient because only two patterns need to be observed, which is like the traditional Misell algorithm. One is an infocus far-field pattern and the other is a defocused far-field pattern. By using the MVFSA to obtain an initial phase guess in the aperture plane which is parameterized by Zernike polynomials, the proposed method can get a better solution than the traditional Misell algorithm and avoid the local stagnation of the traditional Misell algorithm.

The perturbation model and annealing scheme used in the MVFSA are innovative to ensure that the MVFSA can search widely and quickly to approach a rough position near the global minimum.

**Simulation**

To get the amplitude of the far field as the input of the MVFSA-Misell algorithm, a simulation model is built to produce the required data firstly. A model of Shanghai Sheshan-65m-

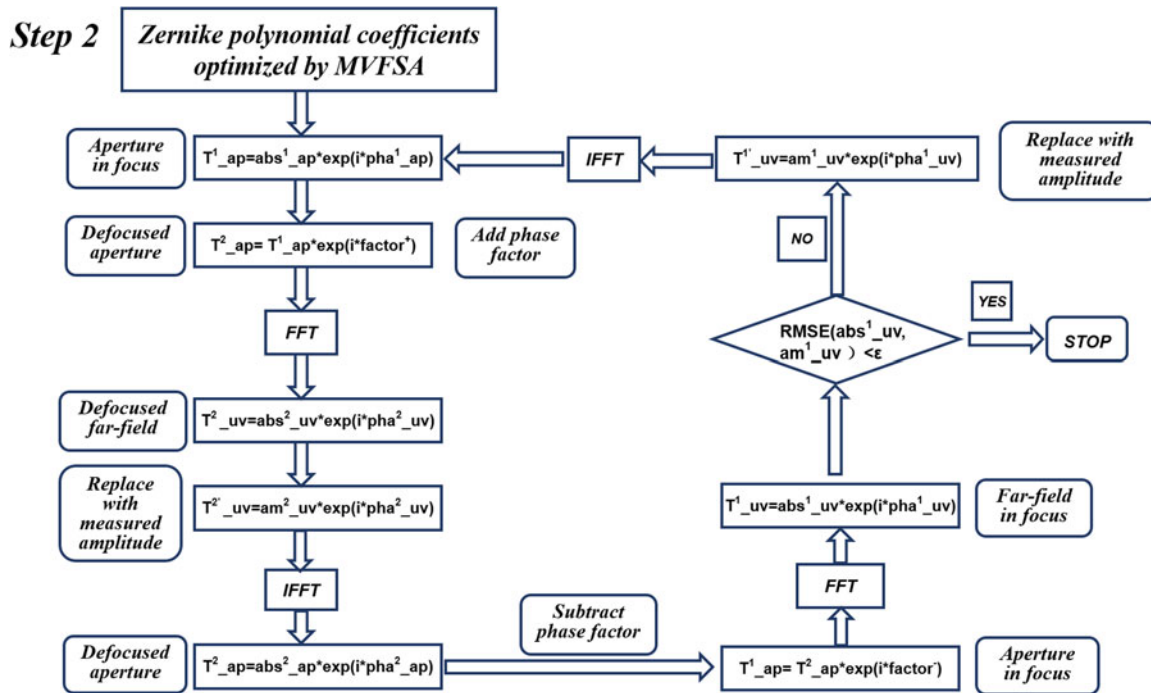


Fig. 3. Flowchart of step 2 of the MVFSA-Misell algorithm.

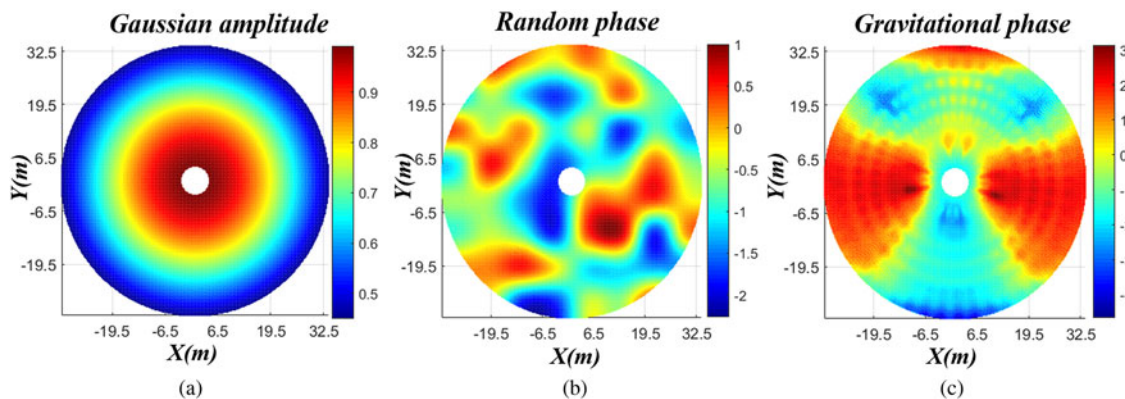


Fig. 4. Original distribution of aperture: (a) amplitude distribution, (b) phase distribution for random distortion, and (c) phase distribution for gravitational distortion.

Table 1. Simulation parameters

Symbol	Meaning	Quantity	Unit
$D$	Diameter of the main reflector	65	m
$d$	Diameter of sub-reflector	6.5	m
$ET$	Edge taper of illumination	-16	dB
$f$	Focal length of the main reflector	20.799	m
$F$	Equivalent focal length	142.62	m
$\lambda$	Wavelength	0.01	m
$ff$	Frequency	30	G
$\Delta d$	Defocusing distance	0.01	m
$N$	Measuring points in the array	64	-
$p$	Oversampling factor	0.5	-

telescope aperture is used to generate infocus and defocused radiation patterns. It is a Cassegrain antenna with a 65 m main reflector and a 6.5 m sub-reflector. The amplitude distribution is the Gaussian type with a -16 dB taper and is blocked by sub-reflector, which is shown in Fig 4(a). The phase distribution simulates two types of surface errors in this paper: one is the random surface error and the other is the gravitational surface error, which is obtained by finite element modelling at EL = 5°. The simulated aperture phase distributions are shown in Figs 4(b) and 4(c).

The real surface deformation can be calculated from the aperture phase distribution by the following equation [1]:

$$\frac{\varepsilon(x, y)}{\lambda} = \frac{1}{4\pi} \sqrt{1 + \frac{x^2 + y^2}{4F^2}} \varphi_{in}(x, y), \tag{17}$$

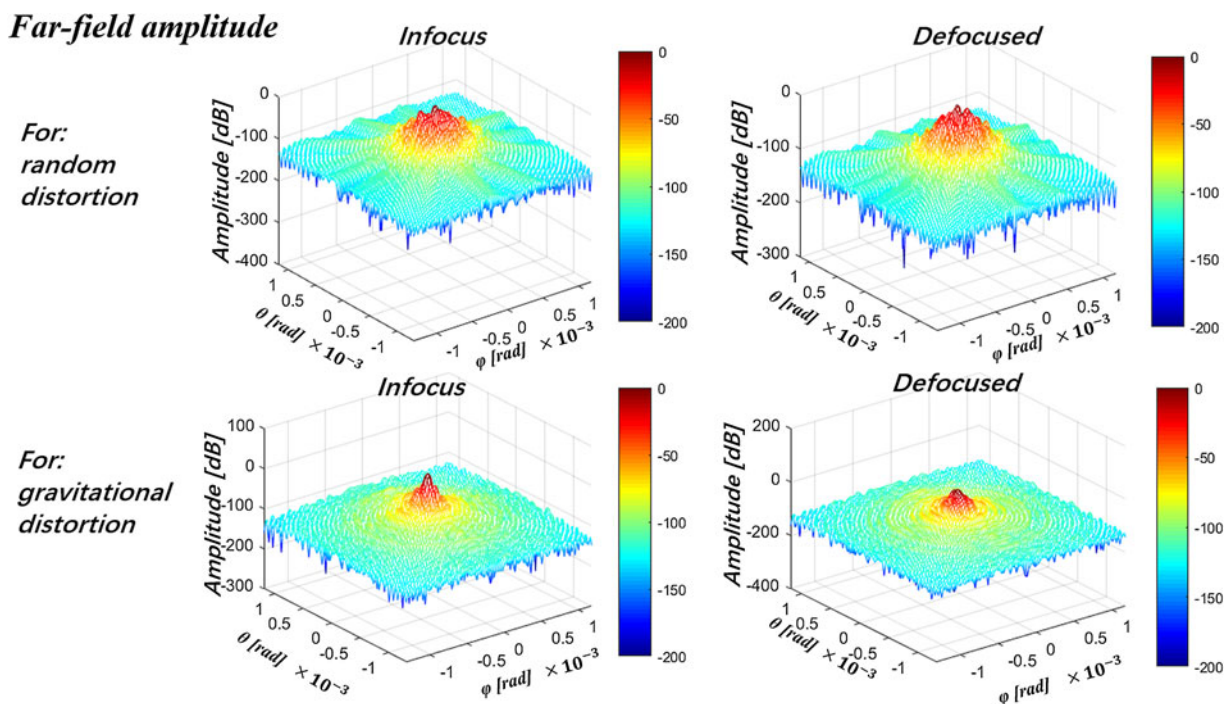


Fig. 5. Simulated far-field amplitudes.

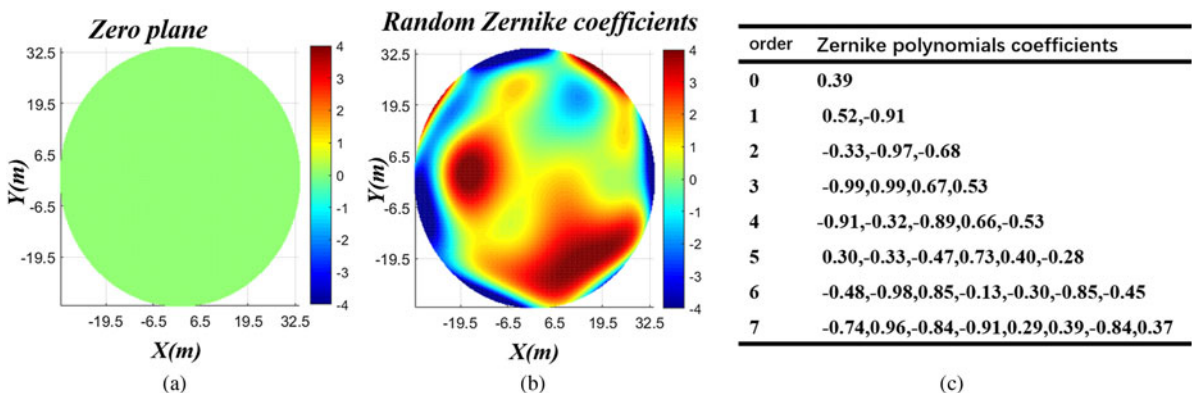


Fig. 6. Simulated initial guesses of in-focus aperture phase. Note that Zernike polynomials coefficients in (c) are for phase guess in (b)

where  $\epsilon(x, y)$  represents the surface distortion,  $\lambda$  is the wavelength,  $\varphi_{in}(x, y)$  represents the phase distribution in the aperture plane in focus, and  $F$  is the focal length of the antenna. The frequency used for simulation in this paper is 30 GHz in the Q band. In this paper, the mean square error of the simulated deformations is both set as 2 mm to reflect the actual situation.

The major simulation parameters are listed in Table 1. As shown in Table 1, the defocusing distance of the sub-reflector was set as 0.01 m, equal to a wavelength, to ensure more than one complete phase rotation across the aperture. The amplitudes of the infocus and defocused far-field amplitudes are shown in Fig. 5. These two amplitudes act as the input of the hybrid MVFSA–Misell algorithm. The output is the phase distribution of the aperture plane in focus. Moreover, the amplitude patterns are supposed to be oversampled by an oversampling factor to avoid the aliasing problem. In this

paper, we set the oversampling factor as 0.5. All calculations were made in  $64 \times 64$  arrays.

For the Misell algorithm, the convergent solution depends on the distance between the initial phase estimation and global minimum. To demonstrate the global search capability of the MVFSA–Misell algorithm, two types of initial phase estimation are used, respectively, one type is the zero plane, and the other type is seventh-order Zernike polynomials with random coefficients between  $-1$  and  $1$ , which are shown in Fig. 6. In the simulation, the population size of the MVFSA is set as 10, and the iterations of stage 1 and stage 2 in the MVFSA are set as 30 and 20, respectively. The convergence criterion used in this paper is defined in (16), and the maximum iterative number is set as 200.

To evaluate the convergence rate and accuracy of the MVFSA–Misell algorithm, we utilize the VFSA, Misell algorithm and

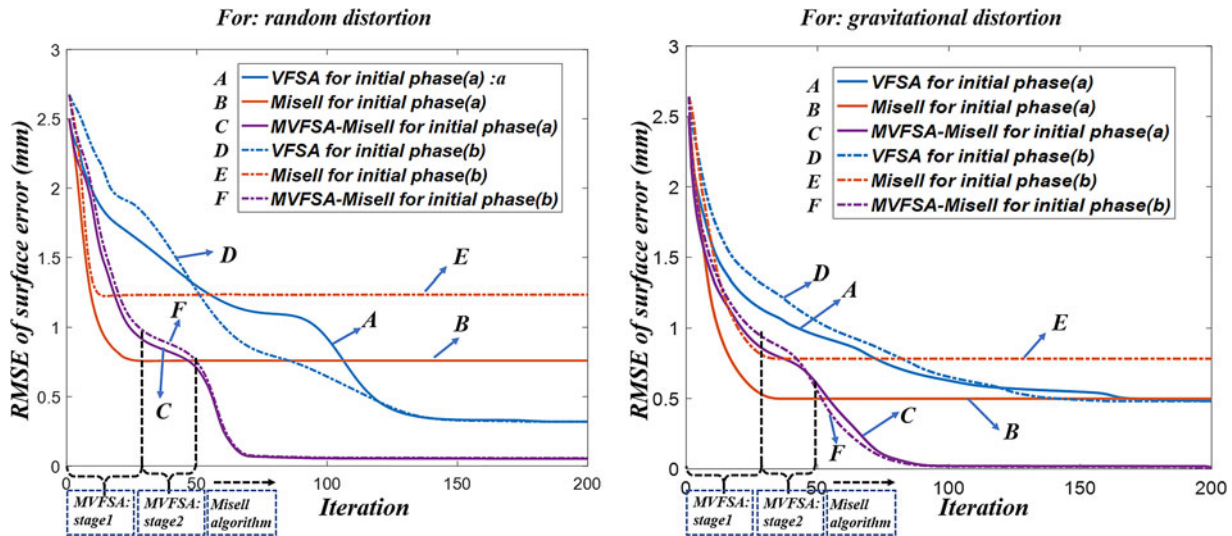


Fig. 7. Convergence curves of VFSA, Misell algorithm and MVFSA-Misell algorithm. Note that the initial phases (a) and (b) are shown in Fig. 6.

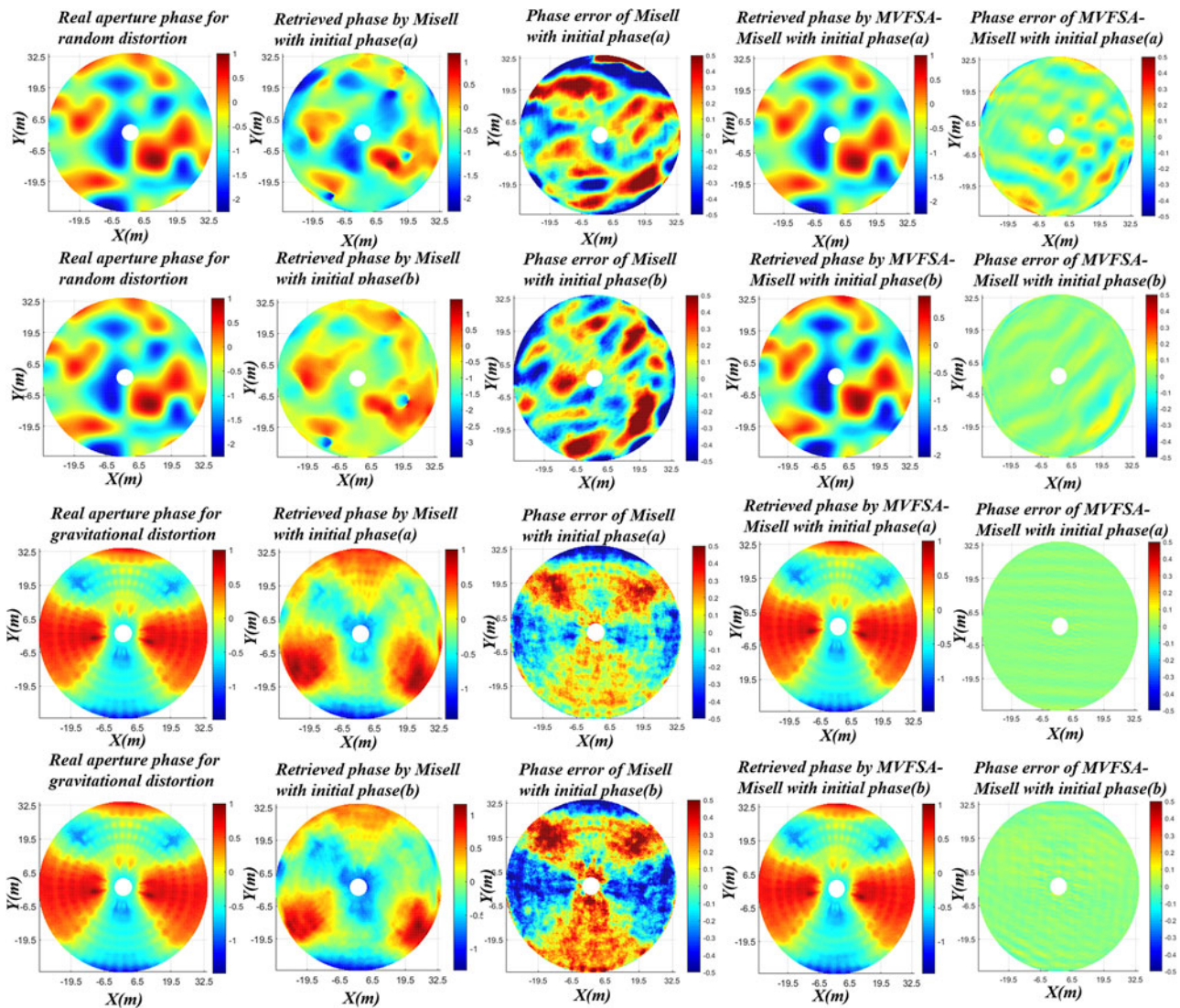


Fig. 8. Convergent solutions of the Misell algorithm and MVFSA-Misell algorithm.

MVFSA–Misell algorithm, respectively, to optimize the simulated phase distribution. The convergence curves of these methods are shown in Fig. 7, and the convergent solutions of these methods are shown in Fig. 8. The RMSE of surface error is defined as follows:

$$RMSE_s = \sqrt{\frac{\sum_N \sum_N (\varepsilon_{ret}(x, y) - \varepsilon_{real}(x, y))^2}{N^2}}, \quad (18)$$

where  $\varepsilon_{ret}(x, y)$  is the retrieved surface distortion of the reflector antenna, and  $\varepsilon_{real}(x, y)$  is the real surface distortion of the reflector antenna.

The analysis of algorithm performance in convergence accuracy and speed is performed in detail according to the simulation results. The analysis is divided into two aspects as below:

- (1) The hybrid MVFSA–Misell algorithm is able to avoid local stagnation of the traditional Misell algorithm. For the simulated random distortion, the surface distortion RMSE of the Misell algorithm is 0.76 mm (error percentage: 38%) under the initial phase (a) and is 1.23 mm (error percentage: 61.5%) under the initial phase (b), while the MVFSA–Misell algorithm converges at the same solution with 0.06 mm RMSE (error percentage: 3%) under the different initial phase estimations. Similarly, for the simulated gravitational distortion, the surface distortion RMSE of the Misell algorithm is 0.5 mm (error percentage: 25%) under the initial phase (a) and is 0.78 mm (error percentage: 39%) under the initial phase (b), while the MVFSA–Misell algorithm converges at the same solution with 0.002 mm RMSE (error percentage: 0.1%) under the different initial phase estimations. It is indicated that the Misell algorithm stagnates at different local minimums due to the difference of initial phases, while the MVFSA–Misell algorithm can converge to the global minimum under different initial guesses, which greatly improved the accuracy of the retrieved surface distortion.
- (2) The hybrid MVFSA–Misell algorithm can greatly accelerate the speed of the traditional VFSA. For the simulated random distortion, the VFSA converges at the 183th iteration (CPU time: 1.2 h) under the initial phase (a) and converges at the 164th iteration (CPU time: 1.08 h) under the initial phase (b), while the MVFSA–Misell algorithm converges at the 72nd iteration (CPU time: 0.33 h) under the different initial phase estimations. For the simulated gravitational distortion, the VFSA converges at the 187th iteration (CPU time: 1.23 h) under the initial phase (a) and converges at the 171th iteration (CPU time: 1.12 h) under the initial phase (b), while the MVFSA–Misell algorithm converges at the 96th iteration (CPU time: 0.35 h) under the different initial phase estimations. The time consumption is decreased by more than 65% through the MVFSA–Misell algorithm. It is also shown in Fig. 7 that the global search capability of stage 1 in MVFSA is higher than that of VFSA, which means the MVFSA can approach a position with a lower cost function in finite iteration steps. In stage 2 of the MVFSA, the RMSE is decreasing continuously and the solution is getting closer to the global minimum. After the limited iteration steps of the MVFSA, the algorithm converts into the Misell algorithm immediately and converges to the final solution with a high speed.

## Conclusion

In this paper, a hybrid global optimization algorithm, named MVFSA–Misell algorithm is proposed to ensure the suppression of the local stagnation of the traditional Misell algorithm. The algorithm is based on the MVFSA, which is a modification of the traditional SA to enhance the global search capability at the beginning of the iteration. By using the MVFSA to optimize the aperture phase distribution parameterized by Zernike polynomial in limited research steps, the Misell algorithm can obtain rough phase estimation near the global minimum. With the rough estimation as an initial phase guess, the Misell algorithm can approach the global minimum with a high speed. Since the MVFSA–Misell algorithm combines the powerful global search capability of MVFSA and the superior speed of local convergence in Misell algorithm, the algorithm is able to converge to the global minimum from different initial phase guesses in a short time.

A simulation has been performed using the prototype model of the Shanghai TM-65m telescope. The digital simulation shows that the MVFSA–Misell algorithm can converge to the global minimum under different initial guesses. The accuracy of the retrieved surface distortion is greatly improved and the convergence time is decreased by more than 65% through the MVFSA–Misell algorithm. In conclusion, the hybrid algorithm is an effective method to solve the local minimum problem of the Misell algorithm and it is probably used in the realistic measurements of the reflector surface.

**Acknowledgement.** This work was supported by the National Basic Research Program of China (973 Program): 2015CB857100.

## References

1. **Rahmat-Samii Y** (1985) Microwave holography of large reflector antennas – simulation algorithms. *IEEE Transactions on Antennas and Propagation* **33**, 1194–1203.
2. **Ruze J** (1996) Antenna tolerance theory – a review. *Proceedings of the IEEE* **54**, 633–640.
3. **Wang W, Li P and Song L** (2009) A method for panel adjustment from far field pattern of large reflector antenna. *Proceedings of the ICMA, Changchun, China*.
4. **Rahmat-Samii Y** (1984) Surface diagnosis of large reflector antennas using microwave holographic metrology: an iterative approach. *Radio Science* **19**, 1205–1217.
5. **Morris D** (1985) Phase retrieval in the radio holography of reflector antennas and radio telescopes. *IEEE Transactions on Antennas and Propagation* **33**, 749–755.
6. **Amineh RK, Mccombe J and Nikolova NK** (2012) Microwave holographic imaging using the antenna phaseless radiation pattern. *IEEE Antennas & Wireless Propagation Letters* **11**, 1529–1532.
7. **Misell DL** (1973) A method for the solution of the phase problem in electron microscopy. *Journal of Physics D (Applied Physics)* **6**, 6–9.
8. **Morris D, Davis JH and Mayer C** (1991) Experimental assessment of phase retrieval holography of radio telescope. *Microwaves, Antennas and Propagation* **138**, 243–247.
9. **Nishibori T, Hirabayashi H, Kobayashi H, Murata Y, Shimawaki Y and Nomura T** (1996) Surface error measurements of large reflector antennas by phase retrieval holography – an application of extrapolation algorithm. *Electronics and Communications in Japan (Part I: Communications)* **79**, 104–114.
10. **Bach U** (2014) Out of Focus Holography at Effelsberg. *Proceedings of the 12th European VLBI Network Symposium and Users Meeting (EVN 2014), Cagliari, Italy*.
11. **Morris D** (1996) Simulated annealing applied to the Misell algorithm for phase retrieval. *IEEE Proceedings in Microwaves, Antennas and Propagation* **143**, 298–303.



12. **Nieto-Vesperinas M, Navarro R and Fuentes FJ** (1988) Performance of a simulated-annealing algorithm for phase retrieval. *Journal of the Optical Society of America A* 5, 30–38.
13. **Zhao L-S, Sen MK, Stoffa P and Frohlich C** (1996) Application of very fast simulated annealing to the determination of the crustal structure beneath Tibet. *Geophysical Journal International* 125, 355–370.



**Yueshu Xu** received his bachelor degree in mechanical engineering from the Shanghai Jiao Tong University in 2015 and started his Ph.D. research at the School of Mechanical Engineering, Shanghai Jiao Tong University in September 2015. His main research interests are microwave holography, phase retrieval algorithm, and reflector surface measurement.



**Qian Ye** received his Ph.D. in 2002 from the Harbin Institute of Technology. He became an associate researcher at Shanghai Jiao Tong University in 2009. His main research interests are microwave holography, phase retrieval algorithm, reflector surface measurement, and large-scale electromechanical system control.



**Guoxiang Meng** received her Ph.D. in 1990 from Xi'an Jiaotong University. She became a full-time professor at Shanghai Jiao Tong University in 2004. Her main research interests are reflector surface measurement, fluid transmission, and control.